

RACORN-1: Adaptive Recall-Preserving Speedup for Low-Selectivity Filtered Vector Search

Yoonseok Kim
Naver Corporation
Seongnam, South Korea
kys910524@gmail.com

Gyusik Choe
Naver Corporation
Seongnam, South Korea
kyusic@gmail.com

ABSTRACT

Filtered Vector Search (FVS), which combines vector embedding similarity with structured metadata predicates, has emerged as a core requirement in RAG and production retrieval systems. ACORN-1, the representative In-filtering algorithm that reuses an existing HNSW index, substantially reduces latency at low selectivity but suffers connectivity instability below 5% selectivity and recall collapse below 1%. We propose **RACORN-1**, an in-place extension of ACORN-1 that resolves this collapse via (i) **Adaptive Search Fallback (ASF)** – repurposing filter-failing nodes as transient bridges to detour around severed paths; bridge and two-hop candidate selection uses stride sampling for spatial diversity. While filter-first ACORN-family methods have a structural recall trade-off relative to distance-first HNSW, RACORN-1 improves the trade-off curve via ASF, minimizing recall loss while substantially reducing latency. Across three 1M-scale and one 40M-scale dataset, RACORN-1 delivers approximately **9–26× latency reduction** over HNSW in the sweet spot (1%–0.3%), and recovers ACORN-1’s recall collapse from 0.45–0.72 (1%) and 0.03–0.10 (0.3%) to 0.70–0.96 and 0.77–0.98 respectively. For the extreme-low-selectivity regime where linear scan can outperform graph search, we combine RACORN-1 with (ii) **Adaptive Exact Fallback (AEF)** in a variant **RACORN-1+**, achieving recall 1.00 with **20–75× speedup** at 1M \leq 0.1% and 13× speedup at 40M 0.01%. Under a Negative Correlation evaluation (K-means clusters), where ACORN-1 collapses (recall 0.08–0.41), RACORN-1 maintains **recall 0.80–0.98 with a 5–9× latency advantage over HNSW**. Together, RACORN-1 and RACORN-1+ form an ACORN-1-compatible mechanism robust to both extreme-low-selectivity and adversarial query-filter correlation.

1 INTRODUCTION

Vector search was initially deployed as pure similarity comparison without metadata filters. In recent production systems and Retrieval-Augmented Generation (RAG) [9] pipelines, however, *hybrid* queries that combine vector embedding similarity with structured metadata predicates (price ranges, stock availability, categories, time windows) have emerged as a core requirement. This requirement is formalized as approximate nearest neighbor search restricted to the subset satisfying the predicate – namely, **Filtered Vector Search (FVS)** [13].

Filtered vector search in HNSW implementations (hnsplib [11], USearch [20], FAISS [3]) operates via **In-filtering**: a predicate check is performed per node during graph traversal – in HNSW, after the distance computation on each visited node. Under this design, latency grows sharply as selectivity decreases, because distance computations on filter-failing nodes accumulate as wasted work.

ACORN-1 [14] addresses this structural inefficiency. ACORN-1 places the predicate check before the distance computation, skipping distance computations on filter-failing nodes; when the number of one-hop predicate-satisfying candidates is insufficient, it dynamically expands to two-hop neighbors (detailed pseudocode in §2.2). This design substantially reduces latency relative to HNSW in the 30%–5% selectivity range. ACORN-1 nevertheless has limits – below 5% selectivity, traversal paths progressively fragment and recall begins to degrade; below 1%, recall collapses. The structural cause of this collapse is that the count of predicate-satisfying candidates in the one-hop and two-hop neighborhoods shrinks proportionally with selectivity, severing traversal paths (analysis in §3).

This paper proposes **RACORN-1 (Resilient ACORN-1)**, which resolves the low-selectivity recall collapse. **Our core insight** is the identification that, in graph-based FVS, *filter-failing nodes are not artifacts to be discarded but reusable resources for connectivity recovery* – by reinterpreting the filter-failing nodes that ACORN-1 discards to avoid distance computation, a design space opens for maintaining a search frontier whose size is independent of selectivity. RACORN-1 realizes this insight as an **in-place extension** of ACORN-1, adding a single core mechanism (i) **Adaptive Search Fallback (ASF)** to the search phase – when one-hop and two-hop predicate-satisfying candidates are insufficient, filter-failing nodes are admitted into the search queue as transient bridges to detour around severed paths (§4.1). Bridge and two-hop candidate selection uses stride sampling to reinforce spatial diversity (§4.2). In §4.4, we derive RACORN-1’s *s*-independent speedup through a region-wise cost analysis, and in §4.5 we provide a formal justification of the *s*-independent expansion-size lower bound under a random graph model. Comprehensive validation is performed in §6–§7 via filter sweeps across four datasets, 21 selectivities, and 12–15 parameter variants per dataset, K-means cluster Positive/Negative Correlation evaluations, and QPS-Recall analysis. We further address the extreme-low-selectivity regime in which graph search becomes inefficient relative to linear scan via a variant **RACORN-1+** that combines RACORN-1 with (ii) **Adaptive Exact Fallback (AEF)** in §5 – when the running predicate-pass ratio falls below a threshold, the system switches automatically to Exact Search.

2 BACKGROUND

Graph-based ANN methods [24] navigate a connected proximity graph by greedy descent toward the query. While we instantiate and evaluate RACORN-1 on HNSW [12] (following ACORN-1 [14]), its core mechanism (ASF) operates at the graph-traversal level and applies in principle to other graph-based ANN methods such as NSG [5].

2.1 HNSW

HNSW is a graph-based ANN data structure organized as a hierarchical Navigable Small World graph, performing greedy traversal at each level and maintaining ef_search candidates at the bottom level to return the K nearest neighbors. At construction, each node is connected to M neighbors ($2M$ at the bottom level by convention); larger $ef_construction$ yields higher-quality neighborhoods.

Given a predicate F , the In-filtering variant (the behavior of hswlib and USearch) modifies the SearchLayer routine of [12] as follows. We maintain a visited set V , a candidate queue C (min-heap by distance to query), and a result queue W (max-heap, capped at ef). We repeatedly extract the nearest node c from C and, for each unvisited neighbor e , register it in V and compute its distance to the query. e enters C if it is closer than W 's furthest, and **enters W only if $F(e)$ is true**. We terminate early once $|W| \geq ef$ and c is farther than W 's furthest. Two key properties follow: (a) **distance computation occurs on every visited node, independent of F** , and (b) **W 's fill target is ef passing nodes, so the visited count grows to approximately ef/s as the selectivity [16] s decreases**.

The unfiltered HNSW search reduces to the routine above with $F(e) \equiv \text{true}$. Upper layers are traversed greedily with $ef=1$, and the routine runs at the bottom layer with $ef=ef_search$, returning the top- K .

2.2 ACORN-1

ACORN [14] adopts a Predicate-Agnostic philosophy and formulates filtered search as *real-time traversal over the Predicate Subgraph — the subgraph induced by predicate-satisfying nodes*. **ACORN-1**, the basis of this work, reuses the existing HNSW graph at construction and performs two-hop dynamic expansion only at search time. Its construction time (TTI) matches HNSW's, with no additional memory cost, making integration with existing systems straightforward.

ACORN-1 reuses HNSW's search structure with two modifications: (a) **only predicate-satisfying nodes** are admitted to the search/result queues, skipping distance computation on filter-failing nodes, and (b) **when one-hop predicate-satisfying candidates are insufficient, two-hop dynamic expansion** augments the candidate set (pseudocode adapted from [14]):

ACORN1-EXPAND, the per-node expansion called in Algorithm 1, behaves as follows. At a visited node u , it first collects the predicate-satisfying one-hop neighbors $C_1 = \{v \in N(u) : F(v) \wedge v \notin V\}$. When $|C_1|$ is insufficient, two-hop expansion gathers the unvisited two-hop predicate-satisfying nodes $C_2 = \{w : w \in N(v), v \in N(u), F(w), w \notin V\}$, capped at M candidates if $|C_2| > M$. The union $C_1 \cup C_2$ is returned.

3 PROBLEM ANALYSIS

3.1 The ACORN-1 Collapse Point

On GIST 1M baseline, ACORN-1's recall and latency profile across selectivities is summarized in Table 1 (see §7.1 for the full 4-dataset baseline).

Two collapse patterns emerge.

Algorithm 1 ACORN-SEARCH-LAYER

Input: query q , filter F , enter point ep , ef

Output: ef closest neighbors to q satisfying F

```

1:  $V \leftarrow \{ep\}$ ;  $C \leftarrow \{ep\}$ 
2:  $W \leftarrow \{ep\}$  if  $F(ep)$  else  $\emptyset$ 
3: while  $|C| > 0$  do
4:    $c \leftarrow$  extract nearest element from  $C$  to  $q$ 
5:    $f \leftarrow$  furthest element from  $W$  to  $q$ 
6:   if  $|W| \geq ef$  and  $dist(c, q) > dist(f, q)$  then
7:     break
8:   end if
9:   for all  $e \in \text{ACORN1-EXPAND}(c, F, V)$  do ▷ (a), (b)
10:     $V \leftarrow V \cup \{e\}$ 
11:     $f \leftarrow$  furthest element from  $W$  to  $q$ 
12:    if  $dist(e, q) < dist(f, q)$  or  $|W| < ef$  then
13:       $C \leftarrow C \cup \{e\}$ 
14:      if  $F(e)$  then ▷ no-op for ACORN-1 (see Sec. 4)
15:         $W \leftarrow W \cup \{e\}$ 
16:        if  $|W| > ef$  then
17:          remove furthest element from  $W$  to  $q$ 
18:        end if
19:      end if
20:    end if
21:  end for
22: end while
23: return  $W$ 

```

Table 1: ACORN-1 collapse vs HNSW on GIST 1M baseline.

Sel	A1 lat (ms)	A1 recall	HNSW lat (ms)	HNSW recall
10%	9.5	0.86	44.8	0.92
5%	6.9	0.81	73.6	0.95
3%	5.2	0.74	108.9	0.95
1%	3.6	0.48	222.4	0.97
0.5%	3.1	0.21	344.8	0.97
0.3%	0.5	0.03	495.5	0.98
0.1%	1.4	0.01	954.0	0.98
0.01%	5.1	0.00	2265.9	0.94

- (1) **Accelerated recall decline below 5%, with a sharp collapse around 1% (0.48)**. As the majority of a visited node's neighbors fail the predicate, even two-hop expansion fails to gather a sufficient number of valid candidates.
- (2) **Recall near zero below 0.3%**. As the majority of two-hop neighbors also fail the predicate, the traversal path is completely severed. Latency remains low, but the results are useless.

On SIFT 1M (128d), the same pattern is observed (1% recall 0.72, converging to zero below 0.1%), though the high-dimensional GIST (960d) exhibits the most extreme collapse.

3.2 Structural Cause

In ACORN-1 search, only predicate-satisfying nodes enter the search queue, to avoid wasted distance computation. From each visited node, predicate-satisfying one-hop neighbors are collected first; two-hop expansion activates only when they are insufficient.

At selectivity s , the expected number of predicate-satisfying one-hop neighbors is approximately $M \cdot s$, and inclusion of two-hop expansion yields only about $M^2 \cdot s$. Below a critical selectivity, even two-hop expansion fails to secure enough predicate-satisfying candidates, the search queue is exhausted, and the traversal path is severed. This is the structural cause of the recall collapse observed in §3.1.

The structural trade-off between filter-first and distance-first: ACORN-family methods adopt a *filter-first* strategy that admits only predicate-satisfying nodes into distance computation. This reduces low-selectivity latency but shrinks the candidate pool relative to the *distance-first* HNSW In-filtering strategy, lowering the recall ceiling. RACORN-1 mitigates this trade-off; §7 quantifies the effect.

3.3 Prior Low-Selectivity Approaches and Their Limits

Existing FVS systems are categorized [13] by when the predicate is processed: **Pre-filtering** (first extract the predicate-satisfying set, then brute-force similarity search over this subset), **Post-filtering** (run ANN search first, then apply the predicate to the result set; `ef_search` must be enlarged to secure enough predicate-satisfying candidates), and **In-filtering** (per-node predicate check during graph traversal). Pre-/Post-filtering has been common in vector databases such as Milvus [22] and AnalyticDB-V [26], but Pre-filtering’s brute-force cost scales with the index size N , and Post-filtering’s search-width overhead grows as selectivity decreases.

This paper addresses the low-selectivity regime within the In-filtering family. Two existing remedies on top of ACORN-1 are **multi-hop expansion** [4, 21] and the **exact-search switch** [21]. Multi-hop expansion raises the hop count to secure additional predicate-satisfying candidates but does not guarantee directional diversity, leaving the traversal at risk of being trapped in a biased path (quantitative comparison in §7.2). The exact-search switch abandons graph search for an exhaustive scan once the predicate-pass rate falls below a threshold; switching too early sacrifices the graph-search latency advantage.

This work adopts the exact-search switch in the form of **Adaptive Exact Fallback (AEF)**, and refers to the variant combining RACORN-1 with AEF as **RACORN-1+** — the detailed switching conditions are summarized in §5.

3.4 Scope and Contribution Boundary

This paper restricts its scope to *in-place enhancements* in the same spirit as ACORN-1 — approaches that reuse an existing HNSW index and improve only the search phase, with no additional build cost or memory. Approaches that incorporate predicate-awareness into the graph construction itself (e.g., Filtered DiskANN [6] — a predicate-aware graph extension of DiskANN [18]; ACORN- γ [14]; NHQ [23]; SeRF [27] for range filtering) incur TTI and memory cost, and are outside our comparison scope. Likewise, **IVF-like cluster/partition-based ANN families** (e.g., Product Quantization [8], ScaNN [7], SOAR [19], SPANN [2]) operate on a different index structure and are outside our scope, since RACORN-1’s mechanism is graph-traversal-level (§4). The adoption of ACORN-1-family methods by production engines such as Weaviate [25],

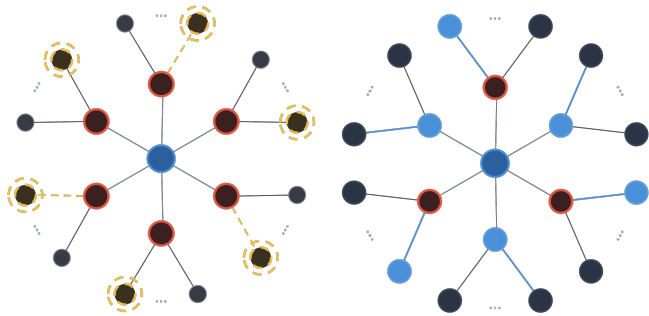


Figure 1: Left: Adaptive Search Fallback (§4.1) — when one-hop predicate-satisfying candidates are insufficient, filter-failing nodes are recruited as transient bridges (yellow dashed) to detour around the severed path. RACORN-1’s core mechanism. Right: Stride sampling (§4.2) — uniform extraction at interval σ from the bridge/two-hop candidate pool, promoting radial spatial diversity. Applied at two call sites in RACORN1-EXPAND.

Lucene/Elasticsearch [4], Vespa [21], and Qdrant [15] supports the operational value of the in-place approach.

3.5 Design Requirements

The analysis above yields two requirements. **R1 (essential)** — provide a detour path when connectivity breaks because the supply of one-hop and two-hop predicate-satisfying candidates is exhausted by decreasing selectivity. **R2 (auxiliary)** — ensure spatial diversity in candidate selection so that the search does not concentrate on a particular one-hop neighbor. Our core proposal in §4, RACORN-1, satisfies **R1 via Adaptive Search Fallback (§4.1)** and **R2 via stride sampling (§4.2)** applied to bridge and two-hop candidate selection.

4 RACORN-1: ADAPTIVE SEARCH FALLBACK

4.1 Adaptive Search Fallback (ASF)

When two-hop expansion still does not produce enough predicate-satisfying candidates, RACORN-1 **admits the collected filter-failing nodes into the search queue as transient bridges** (Figure 1), while **excluding them from the final result set**. That is, the two-hop traversal is split, in a single pass, into two streams: predicate-satisfying candidates (C_2) and a filter-failing bridge pool (B_{pool}). The maximum bridge count (target hereafter) is set to $n \times \text{bridge_ratio}$, where $n = |N(u) \setminus V|$ is the number of unvisited one-hop neighbors of the current node u (V is the visited set of §2.2, and $n \leq M$). The number of bridges actually needed is target minus the number of already-collected **two-hop predicate-satisfying candidates** $|C_2|$. Here `bridge_ratio` is the per-unvisited-one-hop bridge allocation ratio (default 1.0 — one bridge per unvisited one-hop neighbor). The bridge count adapts to both the unvisited one-hop count n and the two-hop predicate-satisfying count $|C_2|$: zero if candidates are sufficient, and growing by the deficit otherwise. Bridges serve as “waypoints to reach valid nodes,” reconnecting severed graph paths.

Intuition for bridge_ratio: within the range $[0, M]$, it acts as a continuous interpolation knob between the behaviors of ACORN-1 and HNSW. As $\text{bridge_ratio} \rightarrow 0$, no bridges are added, and behavior converges to **ACORN-1** (maximum benefit from skipping distance computations on filter-failing nodes, at the cost of low-selectivity recall collapse – §7.1). As $\text{bridge_ratio} \rightarrow M$, most filter-failing nodes within the two-hop region enter the search queue, and behavior approaches **HNSW In-filtering** (bridges as waypoints recover recall, at the cost of HNSW-level distance computation). The default of 1.0 is the minimum BR that defends against ACORN-1’s recall collapse while keeping the distance computation count well below $1/M$ of HNSW’s (§4.4), thereby maximizing the latency advantage.

Visited-set treatment of filter-failing nodes: Outside the ASF branch, RACORN-1 inherits ACORN-1’s behavior – filter-failing nodes are simply skipped from distance computation and not registered in V . Inside the ASF branch ($|C_2| < \text{target}$), however, one-hop and two-hop filter-failing nodes *are* registered in V (see §4.3 pseudocode, ASF branch), because: (i) without this registration, the same failing nodes would re-appear as evaluation candidates in subsequent expansions over the same region, accumulating wasted distance computations; (ii) the selected bridges already secure spatial diversity through stride sampling (§4.2) and continue exploration of the same region, so preserving the unselected nodes is redundant.

ASF activation region: two-hop expansion examines $\sim M^2$ nodes with an expected predicate-pass count $\mathbb{E}[|C_2|] \approx M^2 \cdot s$ (under the regular-graph approximation $n \approx M$). The activation condition $|C_2| < \text{target}$ ($\approx M$ at the default BR=1) corresponds to selectivity $s \lesssim 1/M$ – ASF automatically activates exactly in the region where ACORN-1’s recall begins to collapse. (This $s \lesssim 1/M$ threshold assumes No Correlation; under Pos/Neg query-filter correlation the activation boundary shifts – see §7.5.)

4.2 Stride Sampling

When the available candidate pool P exceeds a target size T , RACORN-1 avoids simply truncating the prefix and instead **samples uniformly at stride** $\sigma = \lfloor |P|/T \rfloor$. Intuition: the two-hop pool is structured as concatenated blocks of each one-hop neighbor v_i ’s two-hop candidates (v_1 ’s two-hop $\rightarrow v_2$ ’s two-hop $\rightarrow \dots$), so prefix truncation could yield a subset biased toward *specific directions*. Stride sampling extracts candidates so that all one-hop neighbors’ two-hop candidates are represented proportionally – i.e., the candidate set exhibits *radial* diversity around the current node.

Stride sampling is invoked at two points in RACORN1-EXPAND (§4.3 pseudocode):

- (1) **Outside ASF (C2 cap):** when one-hop and two-hop predicate-satisfying candidates total $|C_1| + |C_2| > M$, C_2 alone is stride-sampled down to $M - |C_1|$ (C_1 passes through unchanged; Algorithm 2 C2-cap step). This applies whether or not ASF triggers, replacing ACORN-1’s prefix truncation with diversity-preserving extraction.
- (2) **Inside ASF (bridge selection):** when the filter-failing pool $|B_{\text{pool}}|$ exceeds the required bridge count, bridges are selected by stride sampling (Algorithm 2 bridge selection step).

Algorithm 2 RACORN1-EXPAND

Input: node u , filter F , visited set V , result set W , ef
Output: $C_1 \cup C_2$ pass candidates \cup bridges B (bridges excluded from W via filter guard in ACORN-SEARCH-LAYER)

```

1:  $n \leftarrow |\{v \in N(u) : v \notin V\}|$  ▷ unvisited 1-Hop count
2:  $C_1 \leftarrow \{v \in N(u) : F(v) \wedge v \notin V\}$  ▷ 1-Hop pass
3:  $C_2 \leftarrow \emptyset$ ;  $B \leftarrow \emptyset$ ;  $B_{\text{pool}} \leftarrow \emptyset$ 
4: for all  $v \in N(u)$  do
5:   for all  $w \in N(v)$  do
6:     if  $w \in V$  continue ▷ skip visited 2-Hop
7:     if  $F(w)$  then
8:        $C_2 \leftarrow C_2 \cup \{w\}$  ▷ 2-Hop pass
9:     else
10:       $B_{\text{pool}} \leftarrow B_{\text{pool}} \cup \{w\}$  ▷ 2-Hop fail
11:    end if
12:  end for
13: end for
14:  $\text{target} \leftarrow n \cdot \text{bridge\_ratio}$ 
15: if  $|C_2| < \text{target}$  then ▷ Adaptive Search Fallback trigger
16:    $V \leftarrow V \cup \{v \in N(u) : \neg F(v)\}$  ▷ mark 1-Hop fails visited
17:    $V \leftarrow V \cup B_{\text{pool}}$  ▷ mark 2-Hop fails visited
18:   if  $|W| < ef$  then ▷ bridge skip gate when  $W$  full
19:      $\text{needed} \leftarrow \text{target} - |C_2|$ 
20:     if  $|B_{\text{pool}}| > \text{needed}$  then
21:        $B \leftarrow \text{STRIDE-SAMPLE}(B_{\text{pool}}, \text{needed})$ 
22:     else
23:        $B \leftarrow B_{\text{pool}}$ 
24:     end if
25:   end if
26: end if
27: if  $|C_1| + |C_2| > M$  then
28:    $C_2 \leftarrow \text{STRIDE-SAMPLE}(C_2, M - |C_1|)$ 
29: end if
30: return  $C_1 \cup C_2 \cup B$  ▷  $B$  in candidate queue only, not in  $W$ 

```

Both call sites use the same sampling primitive; the quantitative effect of stride over prefix truncation is verified in the §7.4 ablation.

4.3 Pseudocode

(Our implementation supports an optional high-selectivity early-exit on $|C_1|$ sufficiency; we omit it from the pseudocode since this paper’s evaluation focuses on the $\leq 10\%$ region where two-hop always activates.)

RACORN-1 reuses ACORN-SEARCH-LAYER from §2.2 verbatim, replacing the call $\text{ACORN1-EXPAND}(c, F, V)$ with $\text{RACORN1-EXPAND}(c, F, V, W, ef)$ (the additional arguments W and ef are required for the bridge-skip gate decision). The $\text{if } F(e)$ guard in ACORN-SEARCH-LAYER is effectively a no-op for ACORN-1 – whose EXPAND returns only predicate-satisfying candidates – but becomes essential for RACORN-1: it excludes the bridges (whose $F = \text{false}$) returned by RACORN1-EXPAND from the result queue W while still admitting them to the candidate queue C , so they serve their path-reconnection role.

4.4 Cost Analysis

4.4.1 Time Complexity (Base Layer, Small s). The analysis is performed on the base layer under the following assumptions:

Table 2: Time complexity comparison (base layer, small s).

Algorithm	Complexity & Notes
HNSW In-filt.	$O((ef/s) \cdot d + (ef/s) \cdot C)$; $1/s$ inflation.
ACORN-1	$O(ef \cdot d + (ef/s) \cdot C)$; $1/s$ removed from the distance term only (filter-failing nodes skip distance computation); predicate cost per the <i>Simplified C notation</i> below. Valid only while two-hop connectivity holds ($s \geq 1/M$); below this, recall collapses.
RACORN-1	$O(ef \cdot d + ef \cdot M \cdot b \cdot d + (ef/s) \cdot C)$; adds $M \cdot b$ bridges per expansion on top of ACORN-1’s distance term; predicate cost identical. Surface form assumes expansion count = ef .

- The HNSW base layer is a regular graph of degree $\approx M$ (same as A1 in §4.5).
- The predicate F exhibits No Correlation — the pass rate s is independent of the query (same as A2 in §4.5; the effect of Pos/Neg correlation is evaluated separately in §7.5).
- HNSW In-filtering follows the `hnsplib / USearch` implementation — search continues until the result queue is filled with ef predicate-satisfying candidates, so the visited count expands by ef/s .

Notation: d = dimensionality, s = selectivity, C = predicate-evaluation cost (a small constant), M = graph connectivity (base-level degree per §6.2; $M = 2M_{\text{user}} = 32$ at the default $M_{\text{user}} = 16$), N = graph node count, $ef = ef_{\text{search}}$, b = `bridge_ratio` (the §4.1 bridge allocation ratio, default 1.0).

Scope simplification: this analysis focuses on the **distance cost** and uses ef as the expansion-count proxy (abstracting traversal length). Under the per-visit simplification, the resulting M/b ratio matches the empirical **visit-count amplification** (HNSW visits / RACORN-1 visits) — empirically the dominant component of the speedup (see Table 3). The actual *distance-cost ratio* and *latency speedup* differ from M/b by additional factors (per-visit distance count, per-node search overhead) that the model abstracts away, discussed after the table.

Simplified C notation: Table 2 unifies the predicate cost as $(ef/s) \cdot C$ across all three algorithms, but the per-node predicate evaluation count is strictly different — $C_{\text{HNSW}} < C_{\text{RACORN-1}} < C_{\text{ACORN-1}}$. HNSW evaluates F once per visited node; ACORN-1 evaluates F broadly on one-hop and two-hop neighbors and, by not registering failing nodes in V , may re-evaluate them on a re-entry through an adjacent expansion; RACORN-1 registers failing nodes in V inside the ASF branch (§4.3 pseudocode), preventing re-evaluation. The focus of this analysis is the $1/s$ dependence of the distance term, and C is a small constant, so we collapse the notation to a single C .

ACORN-1’s distance computation cost eliminates the $1/s$ factor because filter-failing nodes are skipped, but in the extreme-low-selectivity regime ($s < 1/M$) where two-hop fails to secure M predicate-satisfying neighbors, recall collapses (§3.1). RACORN-1 recovers connectivity at the cost of up to $M \cdot b$ additional distance computations per expansion (target = $n \cdot b$, with $n \leq M$ unvisited one-hop neighbors, hence $\leq M \cdot b$ in §4.1; at the default $b = 1$, $\leq M$

Table 3: Empirical visit-count ratio (§7.1 & §7.6.1; HNSW visits / RACORN-1 visits; BR=1.0 / BR=2.0 per cell, $EF_s = 200$; vs modeled $M/b = 32 \times / 16 \times$).

Selectivity	SIFT 1M	GIST 1M	T2I 1M	T2I 40M
10%	9.4 / 8.9	9.4 / 8.8	9.4 / 8.8	9.3 / 8.9
5%	18.1 / 15.0	18.2 / 15.3	17.7 / 14.6	17.9 / 15.7
1%	35.8 / 21.0	35.3 / 21.0	35.2 / 20.9	39.6 / 24.3
0.5%	36.7 / 20.4	35.2 / 19.5	36.9 / 21.0	42.2 / 24.5
0.1%	30.6 / 16.5	26.6 / 13.8	32.8 / 17.9	41.2 / 22.9
0.05%	25.3 / 13.2	20.2 / 10.2	29.1 / 15.5	39.9 / 22.1
0.01%	19.7 / 9.8	13.9 / 6.2	17.5 / 8.9	36.9 / 20.2

bridges). The total latency is the sum of distance, predicate, and traversal overhead; thus the b -proportional increase in the distance term is diluted in measured latency by the share of the distance term — e.g., switching BR from 1 \rightarrow 2 doubles nominal distance computation, but measured latency in the 1% region increases by only $1.3 \times$ to $1.6 \times$ (§7.6.1).

bridge_ratio extremes (consistent with the §4.1 intuition):

- $b \rightarrow 0$: the distance term reduces to the ACORN-1 form $O(ef \cdot d)$ — s -dependence returns, with low-selectivity recall collapse.
- $b \rightarrow M$: the distance term grows to $O(ef \cdot M^2 \cdot d)$ — approaching HNSW In-filtering cost.

4.4.2 Refinement. The distance term in Table 2 assumed an expansion count of ef , but RACORN-1’s termination condition is the moment W accumulates ef pass results. The average number of passes admitted into W per expansion is $\bar{p} \approx M^2 \cdot s$, so the actual expansion count is

$$N_{\text{exp}} \approx \frac{ef}{M^2 \cdot s}. \quad (1)$$

Since distance computations per expansion are $M \cdot b$ (pass + bridge) and constant, RACORN-1’s total distance cost refines to

$$T_{\text{RACORN-1}}^{\text{dist}} \approx N_{\text{exp}} \cdot M \cdot b \cdot d = \frac{ef \cdot b \cdot d}{M \cdot s}, \quad (2)$$

and its ratio to HNSW’s $ef \cdot d/s$ becomes

$$\frac{T_{\text{RACORN-1}}}{T_{\text{HNSW}}} \approx \frac{b}{M}, \quad (3)$$

a constant **independent of s** . At the default $b = 1$ and $M = 32$, this modeled ratio is $\approx M/b = 32 \times$. Although the formula derives M/b as a *distance-cost ratio* (under the per-visit simplification), measurement shows that M/b also matches the **visit-count amplification** (HNSW visits per RACORN-1 visit) closely — see Table 3 (§7.6.1 BR sweep).

The quantitative accuracy of this formula varies by selectivity region (§7.1 measurement comparison):

- **Upper region ($s \geq b/M$) — outside the formula’s regime:** the combined one-hop and two-hop predicate-pass count $(M + M^2) \cdot s \geq M \cdot b$, so ASF does not trigger and RACORN-1 behaves identically to ACORN-1 (per-expansion distance computations $\approx M^2 \cdot s$, total distance cost $\approx O(ef \cdot d)$ independent of s). The speedup follows the $\approx 1/s$ pattern,

increasing as selectivity drops (visit ratio $\sim 9\times$ at 10%; see Table 3).

- **In-regime** ($\alpha \cdot ef/N \lesssim s \lesssim b/M$) — **matches measurement**: measured visit ratio is essentially flat across selectivity and closely matches M/b — confirming the formula’s “constant speedup” prediction at the visit-count level. Per-dataset variation is a factor of 1.1–1.2 \times across the four datasets (absolute levels in Table 3); selectivity dependence is essentially absent within the in-regime band.
- **Lower region** ($s \lesssim \alpha \cdot ef/N$) — **outside the formula’s regime**: HNSW’s visited count ef/s approaches the graph size N , capping its $1/s$ inflation; the visit ratio thus departs from M/b , falling as HNSW’s visited count flattens toward N while RACORN-1’s continues to grow.

In-regime measurements (1%–0.5%) closely match the modeled M/b at both BR values: BR=1.0 yields visit ratio 35–42 \times (vs $M/b = 32$), and BR=2.0 yields 20–25 \times (vs $M/b = 16$) — confirming that the model’s *visit-count amplification* prediction holds in-regime. Note that the visit count is the per-query traversal length — the quantity §4.4’s Scope simplification abstracted in absolute terms; the empirical match confirms that the M/b model captures the *relative* traversal-length advantage between the two algorithms even without modeling absolute path lengths. The empirical *latency speedup* is attenuated relative to the visit ratio by RACORN-1’s per-expansion search overhead (two-hop scan + ASF logic), which is a roughly dataset-independent per-node cost and does not scale with d . As d grows, distance computation dominates the overhead: GIST ($d = 960$) reaches latency $\sim 26\times$ at 1%; SIFT ($d = 128$) caps at $\sim 10\times$ (overhead fraction larger). In the lower region, visit ratio drops as HNSW saturates to N ; the onset scales with ef/N , so larger- N datasets defer saturation within the eval range.

4.5 Recall Analysis

If §4.4’s cost analysis established an s -independent speedup advantage, this section formalizes the resulting **connectivity preservation** — a necessary condition for the recall stability empirically verified in §7.1. The analysis is performed on the base layer under the following assumptions:

Assumptions:

- (A1) The HNSW base layer is a regular graph of degree $\approx M$ (approximately satisfied in practice).
- (A2) The predicate F exhibits No Correlation — the pass rate s is independent of the query, and predicate-satisfying nodes are uniformly distributed over the graph.
- (A3) `bridge_ratio` $b > 0$ is fixed.

Under (A1) combined with (A2), the predicate-satisfying count among k -hop neighbors of any node u is approximated by Binomial (M^k, s) — i.e., the model is analytically equivalent to a **random regular graph**. The regular degree in (A1) derives from the HNSW graph structure, and the uniform distribution of predicate-satisfying nodes (the randomness needed for analysis) follows from (A2) No Correlation. In what follows, the algorithm’s unvisited one-hop count $n = |N(u) \setminus V|$ is also treated under (A1) with the approximation $n \approx M$ for notational uniformity (the actual algorithm uses per-node n ; §4.3 pseudocode). We use $\text{expand}(u)$ to denote the expansion set returned by EXPAND at node u — for RACORN-1:

$C_1 \cup C_2 \cup B$ (§4.3 RACORN1-EXPAND return); for ACORN-1: $C_1 \cup C_2$ (§2.2 ACORN1-EXPAND prose).

Theorem 1 (s -Independent Lower Bound on RACORN-1 Expansion Size): under assumptions (A1)–(A2), the expected expansion size $|\text{expand}(u)|$ of RACORN-1 at node u satisfies

$$\mathbb{E}[|\text{expand}(u)|] \geq M \cdot b, \quad \text{for } s < b/M. \quad (4)$$

Proofsketch. By §4.1 and §4.3, the expansion size is $|C_1| + |C_2| + |B|$, and on ASF activation, $|B| = \max(0, \min(M \cdot b - |C_2|, |B_{\text{pool}}|))$ (with target $= n \cdot b \approx M \cdot b$). For $s < b/M$, $\mathbb{E}[|C_2|] \approx M^2 \cdot s < M \cdot b$, and $\mathbb{E}[|B_{\text{pool}}|] \approx M^2 \cdot (1 - s) \geq M \cdot b$ (within $s \leq 1 - b/M$; at $M = 32$, $b = 1$, this holds for $s \leq 97\%$). Therefore, in expectation, the deficit $M \cdot b - |C_2|$ is filled by bridges, and $\mathbb{E}[|C_1| + |C_2| + |B|] \geq \mathbb{E}[|C_1|] + M \cdot b \geq M \cdot b$. \square

Theorem 2 (ACORN-1 Expansion Vanishing): under assumptions (A1)–(A2), in ACORN-1 (which omits bridges), $|\text{expand}(u)| = |C_1| + |C_2|$, and

$$\mathbb{E}[|\text{expand}(u)|] \approx M \cdot s \cdot (1 + M) \rightarrow 0 \quad \text{as } s \rightarrow 0. \quad (5)$$

That is, ACORN-1’s expected expansion size shrinks to zero with selectivity, whereas RACORN-1’s stays $\geq M \cdot b$ by Theorem 1.

Together, Theorems 1 and 2 establish the **connectivity preservation** distinction: for $s < b/M$, RACORN-1’s traversal frontier does not stall (even in the $s \rightarrow 0$ limit), while ACORN-1’s frontier stall is intrinsic.

This structural difference is empirically confirmed in §7.1 by RACORN-1’s s -independent recall stability (SIFT 1M baseline 0.96–0.99) versus ACORN-1’s recall collapse (0.72 \rightarrow 0).

Empirical validation (cross-reference to §7.1):

- SIFT 1M baseline, $s \in \{1\%, 0.5\%, 0.1\%, 0.01\%\}$:
 - ACORN-1 recall: 0.72 \rightarrow 0.40 \rightarrow 0.01 \rightarrow 0.00 (converging to zero as $s \rightarrow 0$, consistent with Theorem 2).
 - RACORN-1 recall: 0.96 \rightarrow 0.97 \rightarrow 0.99 \rightarrow 0.98 (maintained within the s -independent range 0.96 \sim 0.99, consistent with Theorem 1).
- GIST, T2I 1M and 40M exhibit the same pattern (§7.1 and §7.2).

This analysis shows that RACORN-1’s core design decision — **repurposing filter-failing nodes as bridges** — structurally removes selectivity dependence. ACORN-1’s recall collapse is the direct consequence of expansion stall ($|\text{expand}(u)| \rightarrow 0$, Theorem 2), and is essentially unavoidable while preserving the algorithmic skeleton in which only predicate-satisfying nodes enter the search queue.

5 RACORN-1+: COMPLEMENTING ACORN-1 WITH ADAPTIVE EXACT FALLBACK

RACORN-1 achieves an order-of-magnitude latency reduction over HNSW across most of the extreme-low-selectivity regime while substantially recovering recall relative to ACORN-1 (§4.4 and §7.1), but at extreme low selectivity graph search becomes slower than linear scan (Exact Search) — HNSW saturates to visiting all N nodes in this regime (§4.4 lower region), and RACORN-1’s own bridge cost (distance computation on some filter-failing nodes) compounds with its uncapped $1/s$ -growing traversal length. Linear

scan computes distance only over predicate-satisfying nodes ($N \cdot s$), so its cost is bounded by $N \cdot s \cdot d$. In this regime, abandoning graph search and switching automatically to Exact Search — via the **Adaptive Exact Fallback (AEF)** mechanism — is operationally effective; we refer to RACORN-1 combined with AEF as **RACORN-1+**.

Specifically, after a sufficient number of visited nodes has been collected, the running predicate-pass ratio (the fraction of predicate-satisfying nodes among the visited) is measured, and when it falls below a threshold, the system switches to Exact Search. After the switch, Pre-filtering (§3.3) guarantees recall 1.0. AEF itself is an option provided by Vespa (§3.3), but **RACORN-1+**'s AEF reuses the running-selectivity signal that RACORN-1's ASF emits at every expansion as its trigger — sampling occurs only when ASF fires, and inside the branch the filter-failing nodes are also registered in V (§4.3), so the pass rate is measured more accurately than in standalone ACORN-1 (which omits this V registration). Moreover, ASF activates only in the extreme-low-selectivity regime, so AEF's monitoring and switch decision are naturally restricted to that region, yielding an efficient operation targeted within the integration with RACORN-1.

Observed RACORN-1+ exact-switch onset selectivity ($M = 16$, $EF_s = 200$; the first selectivity at which exact switch activation improves recall/latency over RACORN-1): 1M datasets (SIFT / GIST / T2I) $\sim 0.3\%$, T2I 40M $\sim 0.01\%$ (onset table in §7.3). Below 0.1% on 1M datasets, RACORN-1+ simultaneously achieves recall 1.00 and 20–75 \times speedup (§7.3 at $EF_s = 200$ baseline). On 40M, since the AEF FB threshold is 1/10 of 1M's, the exact switch activates only at deeper selectivities.

AEF FB Threshold parameter: the AEF activation threshold (AEF FB Threshold) is a user-set parameter. In our experiments, we use 0.003 (0.3%) at 1M and 0.0003 (0.03%) at 40M, both at $EF_s = 200$. **Why the 40M threshold is 1/10 of the 1M threshold — a cost-benefit argument:** on AEF activation, the brute-force cost is the sum of the predicate scan over all N nodes and the distance evaluation over the $N \cdot s$ predicate-satisfying nodes — both proportional to N . At 40M, 0.1%, the brute-force latency is $\sim 10\times$ RACORN-1's graph search latency — in the region where graph search is favorable, triggering AEF would be a loss. Lowering the threshold restricts AEF activation to selectivities where brute-force is genuinely favorable (a 1.6 \times advantage at 40M, 0.01%; §7.3). The proportional $N \uparrow \Rightarrow$ threshold \downarrow scaling is a direct consequence of this cost-benefit balance. The measured appropriate threshold also scales with EF_s — at $EF_s = 400$, the appropriate values are $\sim 0.6\%$ (1M) and $\sim 0.06\%$ (40M), both doubled. We adopt a user-specified threshold in this paper; automatic determination based on N and EF_s (closed-form formulation or dynamic calibration from operational statistics) is left as future work (§8(2)).

The empirical RACORN-1+ AEF results (latency and recall effects in the cross-over region) are reported in §7.3.

6 EXPERIMENTAL SETUP

6.1 Datasets

Each dataset consists of N vectors (dimension D) and n_q queries (Table 4). We use SIFT 1M and GIST 1M [8], and Text2Image 1M / 40M [17].

Dataset characteristics (the origin of the difference in ACORN-1's collapse pattern in §3.1 and §7.1): SIFT 1M and GIST 1M are *in-distribution* (base and query from the same distribution via hold-out), with GIST's high dimensionality (960d) invoking the **curse of dimensionality**. Text2Image 1M / 40M is **cross-modal** (image-embedding base, text-embedding query), inducing a **modality gap**; the 40M variant additionally introduces large-scale effects.

Table 4: Datasets used in evaluation.

Dataset	N	D	Metric	n_q
SIFT 1M	1,000,000	128	L2	992
GIST 1M	1,000,000	960	L2	992
Text2Image 1M	1,000,000	200	Cosine	992
Text2Image 40M	40,000,000	200	Cosine	992

6.2 Implementation and Environment

We extend USearch (an open-source HNSW library) to implement ACORN-1 and RACORN-1 within a single binary; the HNSW baseline uses USearch HNSW + In-filtering. ACORN-1 and RACORN-1 operate on the base level (§2.1: $2M = 32$ connections per node). For brevity in subsequent analysis and notation, degree is denoted simply as M . Hardware is AMD EPYC 7543 $\times 2$ (64 cores), RAM 1 TB (PC4-3200AA-R 32GB $\times 32$); the OS is Red Hat Enterprise Linux 8.6, with builds via g++ 14.2.1 + -O3 -DNDEBUG.

6.3 Common Parameters

$K = 100$, bridge_ratio (BR) = 1.0, $M = 16$ (HNSW construction parameter; base-level degree $2M = 32$, denoted simply as M in §4.4/§4.5 per §6.2), $EF_c = 100$, $EF_s = 200$, search threads = 32 (NUMA-aware), Runs = 10 (2-level median), Warmup = 1. **Unless otherwise noted, the baseline values above are used.** Per-evaluation variants (BR sweep, EF_s sweep, m32, efc500, 3-hop, etc.) are defined in the introduction of each §7.x subsection.

6.4 Selectivity Grid and Query Correlation

21 selectivity buckets: 100%, 90%, 70%, 50%, 30%, 20%, 10%, 5%, 4%, 3%, 2%, 1%, 0.8%, 0.6%, 0.5%, 0.4%, 0.3%, 0.2%, 0.1%, 0.05%, 0.01%. We evaluate all three Query Correlation conditions — the primary evaluation uses **No Correlation** (query-independent modulo predicate, a neutral evaluation condition); §7.5 covers two additional conditions, **Positive** and **Negative Correlation** based on K-means clustering; and §7.6.2 measures BR sensitivity under negative correlation.

The predicate F in our experiments is implemented as a **modulo operation over node IDs**, chosen because (i) it is deterministic for a given ID, ensuring reproducibility; (ii) it is an $O(1)$ operation negligible relative to distance computation, simplifying cost analysis around the distance term; and (iii) selectivity can be controlled exactly by adjusting the modulo divisor.

6.5 Measurement Protocol

For each (case \times selectivity), 10 measurements are taken and a 2-level median is reported. Recall is the Top-K intersection ratio

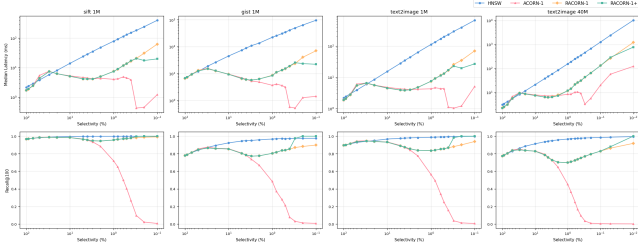


Figure 2: Baseline 4-way comparison across the four datasets.

against exact ground truth. Latency is the per-query mean latency (32 threads, NUMA-aware, 992 queries — with 32 threads under equal partitioning).

7 EVALUATION

Four datasets \times HNSW \cdot ACORN-1 \cdot RACORN-1 \cdot RACORN-1+ — a 4-way comparison. Chart selectivity ranges are 100%–0.1% for 1M and 100%–0.01% for 40M (a subset of the 21 buckets in §6).

Recall baseline and comparison framing: HNSW and the ACORN family embody distinct design philosophies — *distance-first* (HNSW; filter-after-graph) and *filter-first* (ACORN-1, RACORN-1; filter-aware traversal). At low selectivity, HNSW’s distance-first traversal incurs heavy latency but maintains high recall on the small filter-passing set (even as the set shrinks), whereas filter-first methods cap traversal cost — yielding the family’s characteristic latency advantage — at the cost of a lower recall ceiling (cf. §3.2). Accordingly, our primary recall claim is the **ACORN-1 \rightarrow RACORN-1 recovery**: RACORN-1 closes ACORN-1’s low-selectivity recall collapse while preserving the filter-first latency edge, not parity with HNSW. The reporting protocol that operationalizes this view — using HNSW@selectivity=100% recall (minus a 1%p tolerance) as a guardrail RACORN-1+ maintains across all selectivities — is detailed in §7.8.

7.1 Overall Performance: HNSW vs ACORN-1 vs RACORN-1 vs RACORN-1+

Under the baseline setting ($M = 16$, $EF_c = 100$, $EF_s = 200$, $BR=1.0$), latency and recall of the four modes are measured at nine selectivity buckets (10 / 5 / 3 / 1 / 0.5 / 0.3 / 0.1 / 0.05 / 0.01%).

Figure 2 shows the Pareto curves across the four datasets, and Table 5 reports speedup \times recall (in parentheses) relative to HNSW for ACORN-1 / RACORN-1 / RACORN-1+. HNSW recall ranges 0.92–1.00 across all regions (SIFT / T2I 1M 0.99+, GIST 0.92–0.98, T2I 40M 0.94–0.98). Bold recall marks the ACORN-1 collapse; for cells with recall ≤ 0.5 , speedup is meaningless and is reported as “—”.

Above 3% selectivity, the three modes behave nearly identically — neither fallback nor exact switch is triggered — and RACORN-1 / RACORN-1+ deliver 2.7–19 \times speedup over HNSW. The picture shifts in the **1%–0.3% sweet spot**, where ACORN-1’s recall begins collapsing to 0.45–0.72 while RACORN-1’s ASF recovers it by +0.24 to +0.32 at 1% and +0.74 to +0.88 at 0.3%; peak speedup reaches 26 \times on GIST at 1%, with T2I 1M / 40M attaining 15 \times / 11 \times at 0.5%. The RACORN-1+ exact switch begins partial activation around 0.3%

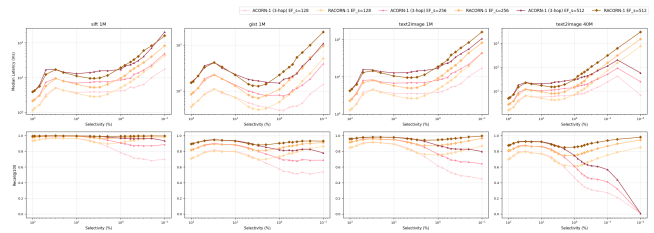


Figure 3: RACORN-1 vs ACORN-1 3-hop across four datasets.

on 1M (recall 0.87–0.98 \rightarrow 0.97–1.00) and becomes decisive below 0.1%, sustaining recall **1.00** with **20–75 \times speedup** (peak 75 \times on GIST at 0.01%); RACORN-1 alone yields 5–14 \times speedup with recall maintained at 0.81–1.00 as HNSW saturates to its N -cap (§4.4 lower region). On T2I 40M, the AEF threshold delays activation until 0.01%, where RACORN-1+ fully kicks in (recall 1.00, **13 \times speedup**; RACORN-1 attains 8.4 \times).

7.2 RACORN-1 vs ACORN-1 with 3-Hop Expansion

In §3.3 we argued qualitatively that multi-hop expansion (3-hop) does not guarantee directional diversity even when it increases the quantitative candidate count, and may be trapped in a biased traversal path. This section verifies the claim through a head-to-head comparison at $EF_s = 256$ (other parameters per §6 baseline): **ACORN-1 (3-hop)** with 3-hop expansion only, against **RACORN-1** with two-hop expansion + ASF fallback.

Figure 3 compares RACORN-1 against the ACORN-1 3-hop variant across the four datasets. At selectivity $\geq 5\%$ the two algorithms are nearly equivalent (Δ recall ≤ 0.02) — candidate quantity is sufficient. From 1% down to 0.1% the 3-hop variant’s recall drops by 0.05–0.42 (SIFT -0.05 to -0.12 ; GIST -0.09 to -0.21 ; T2I 1M -0.07 to -0.30 ; T2I 40M -0.09 to -0.42), and at 0.05% and below it collapses sharply (SIFT 0.05% to 0.77, then essentially zero at 0.01%: 0.01–0.03 across all datasets). The interpretation is structural: 3-hop expansion enlarges the graph reach to increase the candidate count, but at extreme low selectivity even within the expanded reach the predicate-satisfying candidates themselves are insufficient or directionally skewed. RACORN-1’s fallback employs a different mechanism — repurposing filter-failing nodes as transient bridges (§4.1) — that bypasses this limit. The two recovery strategies are thus **fundamentally different and cannot be substituted by simply increasing hop count**.

7.3 RACORN-1+ AEF Effect (Exact Switch Activation)

This section quantifies the Adaptive Exact Fallback (AEF) of RACORN-1+ that was qualitatively introduced in §5. The central question: *at what selectivity does the exact switch activate, and what is its effect relative to RACORN-1 alone?* The AEF FB Threshold is 0.003 at 1M and 0.0003 at 40M ($EF_s = 200$; in QPS sweeps, the threshold is dynamically scaled proportionally to ef_search — see §7.8); other parameters follow the §6 baseline.

Table 6 reports the AEF onset selectivity together with the recall/speedup change at onset across datasets: 1M datasets exhibit

Table 5: Speedup \times (recall) vs HNSW across selectivity, 4-way comparison.

Dataset / Mode	10%	5%	3%	1%	0.5%	0.3%	0.1%	0.05%	0.01%
sift 1M ACORN-1	2.6 \times (0.98)	5.1 \times (0.97)	8.4 \times (0.93)	19.6 \times (0.72)	— (0.40)	— (0.10)	— (0.01)	— (0.00)	— (0.00)
sift 1M RACORN-1	2.7 \times (0.98)	5.7 \times (0.97)	8.5 \times (0.95)	10.4 \times (0.96)	9.5 \times (0.97)	8.9 \times (0.98)	6.4 \times (0.99)	5.6 \times (0.99)	5.2 \times (0.98)
sift 1M RACORN-1+	2.7 \times (0.98)	5.7 \times (0.97)	8.5 \times (0.95)	10.6 \times (0.96)	9.5 \times (0.97)	8.9 \times (1.00)	20.2\times (1.00)	28.7\times (1.00)	51.1\times (1.00)
gist 1M ACORN-1	4.7 \times (0.86)	10.7 \times (0.81)	20.9 \times (0.74)	— (0.48)	— (0.21)	— (0.03)	— (0.01)	— (0.00)	— (0.00)
gist 1M RACORN-1	4.8 \times (0.85)	11.4 \times (0.80)	19.2 \times (0.77)	25.9\times (0.80)	22.9 \times (0.84)	21.1 \times (0.87)	13.7 \times (0.90)	10.2 \times (0.90)	7.3 \times (0.81)
gist 1M RACORN-1+	4.8 \times (0.85)	11.4 \times (0.80)	19.2 \times (0.77)	26.6 \times (0.80)	22.7 \times (0.84)	19.6 \times (0.97)	43.3\times (1.00)	49.3\times (1.00)	75.0\times (1.00)
t2i 1M ACORN-1	3.2 \times (0.93)	6.5 \times (0.89)	11.0 \times (0.84)	26.0 \times (0.56)	— (0.25)	— (0.04)	— (0.00)	— (0.00)	— (0.00)
t2i 1M RACORN-1	3.4 \times (0.93)	7.2 \times (0.89)	11.0 \times (0.86)	15.0 \times (0.84)	15.0 \times (0.86)	11.4 \times (0.88)	9.5 \times (0.94)	8.1 \times (0.97)	5.8 \times (1.00)
t2i 1M RACORN-1+	3.4 \times (0.93)	7.2 \times (0.89)	11.1 \times (0.86)	15.0 \times (0.84)	15.0 \times (0.86)	12.9 \times (0.98)	24.6\times (1.00)	38.6\times (1.00)	61.8\times (1.00)
t2i 40M ACORN-1	2.7 \times (0.83)	5.3 \times (0.79)	8.1 \times (0.72)	— (0.45)	— (0.17)	— (0.03)	— (0.00)	— (0.00)	— (0.00)
t2i 40M RACORN-1	2.8 \times (0.83)	6.0 \times (0.79)	8.9 \times (0.73)	13.3 \times (0.70)	11.4 \times (0.74)	10.7 \times (0.77)	9.7 \times (0.83)	9.0 \times (0.86)	8.4 \times (0.92)
t2i 40M RACORN-1+	2.8 \times (0.83)	6.0 \times (0.79)	9.3 \times (0.73)	13.1 \times (0.70)	11.3 \times (0.74)	10.7 \times (0.77)	9.7 \times (0.83)	8.3 \times (0.88)	13.1\times (1.00)

Table 6: RACORN-1+ exact-switch onset across datasets.

Dataset	sel	recall (R-1 \rightarrow R-1+)	speedup vs HNSW
sift 1M	0.3% (onset)	0.98 \rightarrow 1.00	8.9 \times \rightarrow 8.9 \times
sift 1M	0.1%	0.99 \rightarrow 1.00	6.4 \times \rightarrow 20.2\times
gist 1M	0.3% (onset)	0.87 \rightarrow 0.97	21.1 \times \rightarrow 19.6 \times
gist 1M	0.1%	0.90 \rightarrow 1.00	13.7 \times \rightarrow 43.3\times
t2i 1M	0.3% (onset)	0.88 \rightarrow 0.98	11.4 \times \rightarrow 12.9 \times
t2i 1M	0.1%	0.94 \rightarrow 1.00	9.5 \times \rightarrow 24.6\times
t2i 40M	0.01% (onset)	0.92 \rightarrow 1.00	8.4 \times \rightarrow 13.1\times

partial activation from 0.3% and full activation below 0.1% (recall 1.00). On 40M, the AEF FB threshold is 1/10 that of 1M, so onset is delayed to 0.01%.

All 1M datasets exhibit first partial activation at 0.3% (recall \geq 0.97), the point at which the 1M AEF FB threshold (0.003) is reached. Below 0.1% the exact switch yields a latency reduction as well: RACORN-1’s graph-search cost grows as $1/s$ (§4.4) while RACORN-1+’s exact switch caps cost at brute-force ($N \cdot s \cdot d$), constant — resulting in a **2.6–10.6 \times latency reduction over RACORN-1** while guaranteeing recall 1.0 (R1+/R1 speedup ratio: 2.6–3.2 \times at 0.1%, 9.9–10.6 \times at 0.01%; see consolidated table in §7.1). On 40M, the AEF FB threshold (0.0003) is 1/10 of 1M’s, so the exact switch is not activated until deeper selectivities — activation at 0.01% yields recall 1.00 with 13 \times speedup. The cost-benefit rationale for the 40M’s 1/10 ratio is given in the AEF FB Threshold paragraph of §5.

7.4 Stride Sampling Ablation

The decisiveness of ASF (§4.1), RACORN-1’s core mechanism, is directly established by the §7.1 baseline: RACORN-1’s ASF-OFF behavior is equivalent to ACORN-1 at BR=0 (the fallback-deactivation flag), so the §7.1 ACORN-1 vs RACORN-1 recall delta (1%: +0.24 to +0.32; 0.3%: +0.74 to +0.88) is precisely ASF’s standalone contribution. Without ASF, recall regresses to ACORN-1’s collapse level, as the §7.1 measurements confirm.

This section isolates the recall effect of **stride sampling** (§4.2) by comparing RACORN-1 default (stride ON) against a stride_off variant (other parameters per §6 baseline). The stride_off variant

replaces stride sampling with prefix truncation at both call sites (bridge selection inside ASF; C2 cap).

Stride’s standalone effect is most meaningful on T2I within our measurements: SIFT 1M (L2, 128d) and GIST 1M (L2, 960d) yield $|\Delta\text{recall}| \leq 0.006$ (noise level), T2I 1M (cosine, 200d) shows -0.016 to -0.019 at 1%–0.5%, and **T2I 40M (cosine, 200d) shows the largest effect, -0.028 to -0.042 at 1%–0.5%**. The distributional characteristics of cosine embeddings could be more sensitive to the directional diversity of fallback bridges, with the large-scale variant (40M) appearing more affected than 1M. Combined with the §7.1 ACORN-1 vs RACORN-1 baseline, this stride ablation cleanly separates the two mechanism contributions: **the $M \cdot b$ expansion-size lower bound in the §4.5 analysis is guaranteed by ASF**, while stride sampling (§4.2) provides a smaller, cost-free auxiliary recall gain on top.

7.5 Query Correlation Effect (Pos/Neg)

In addition to the §6 No Correlation modulo predicate, this section measures the effect of **query-filter correlation (Pos/Neg)** on the ACORN family. We introduce a cluster-based predicate — assigning a K-means [10] cluster_id to each node, then **positive**: target = query’s cluster_id (predicate-satisfying nodes lie near the query); **negative**: target \neq query’s cluster_id (a deterministic-seed selection of a different single cluster; predicate-satisfying nodes lie far from the query). Both modes preserve selectivity at $\sim 1/K$, but the spatial distribution of surviving nodes is semantically different.

We measure two scenarios (K=10 with sel \sim 10%, K=100 with sel \sim 1%) \times 4 datasets with ef \in {128, 256, 384, 512} (BR=1.0; other parameters per §6 baseline).

Figure 4 integrates K=10 and K=100 Pareto curves under both Pos and Neg correlation across the four datasets. At efs=256, the three algorithms diverge sharply under negative correlation. **HNSW’s latency explodes** because graph traversal becomes inefficient: K=100 negative latencies escalate to SIFT 615 ms, GIST 1237 ms, T2I 1M 501 ms, and **T2I 40M 8691 ms (= 8.7 s)**, while recall is largely preserved (0.87–0.99) — eligible nodes lie far from the query, so query-directed greedy traversal must pass through ineligible regions to reach them, inflating the visited count and accumulating per-node distance computations. **ACORN-1 alone becomes**

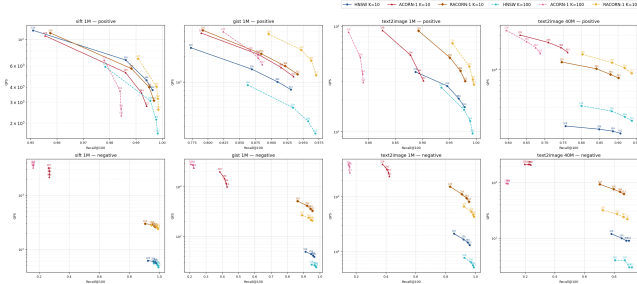


Figure 4: Pareto curves under Pos vs Neg correlation, $K=10/100$ integrated.

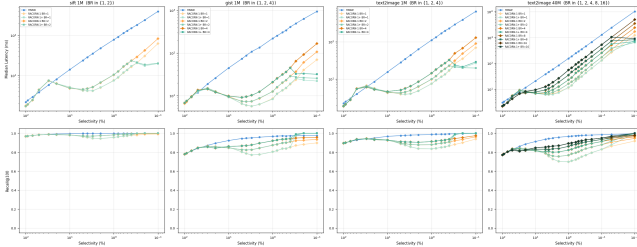


Figure 5: BR sweep under No Correlation across four datasets.

unusable: $K=100$ recall collapses to SIFT **0.161** (from 0.984), GIST **0.221** (from 0.867), T2I 1M **0.156** (from 0.785), and T2I 40M **0.080** (from 0.651), because two-hop expansion alone cannot reach eligible nodes when both one-hop and two-hop reside in the query’s cluster region. **RACORN-1’s ASF acts as the safety net:** recall is preserved at 0.82–0.98 with a 5–9 \times latency advantage over HNSW (SIFT $K=100$ 5 \times , GIST 9 \times , T2I 1M 8 \times , T2I 40M 7 \times) – fallback directly explores the query-uncorrelated eligible pool and prevents expansion stall, consistent with §4.5 Theorem 1’s mechanism (bridges preserve $|C_2| \geq Mb$ regardless of where eligible nodes lie).

The $K=10$ setting (sel $\sim 10\%$) exhibits a latency-recall pattern comparable to $K=100$ ($\sim 1\%$) – e.g., SIFT $K=10$ negative HNSW latency ~ 533 ms with ACORN-1 recall 0.27 – confirming that **correlation is a determining variable on par with selectivity**. Finally, the BR sensitivity pattern reverses under negative correlation: BR \downarrow becomes the efficient frontier, quantified in §7.6.2.

7.6 RACORN-1 Bridge Ratio (BR) Sensitivity

In §4.1, BR was proposed as a continuous interpolation knob over $0 \leq BR \leq M$. This section sweeps BR to measure the recall-latency trade-off and recommended values – §7.6.1 covers BR \uparrow under No Correlation (default operational scenario); §7.6.2 covers BR \downarrow under negative correlation (an adversarial scenario with a counter-intuitive pattern). (BR=0 disables fallback and is equivalent to ACORN-1 – see §7.1 baseline; this section restricts attention to $BR > 0$.)

7.6.1 No Correlation BR Sweep. Figure 5 sweeps BR across the four datasets, and Table 7 reports the recall change from BR=1 to per-dataset BR $_{\max}$ at 1% selectivity.

Table 7: BR=1 \rightarrow BR $_{\max}$ recall change at 1% selectivity.

Dataset	BR set	BR=1 (lat)	BR $_{\max}$ (lat)	Δ recall
SIFT 1M	{1, 2}	0.96 (7.5 ms)	0.98 (10.4 ms)	+0.02
GIST 1M	{1, 2, 4}	0.80 (8.6 ms)	0.92 (20.8 ms)	+0.12
T2I 1M	{1, 2, 4}	0.84 (7.4 ms)	0.91 (14.3 ms)	+0.07
T2I 40M	{1, 2, 4, 8, 16}	0.70 (11.8 ms)	0.89 (55.5 ms)	+0.19

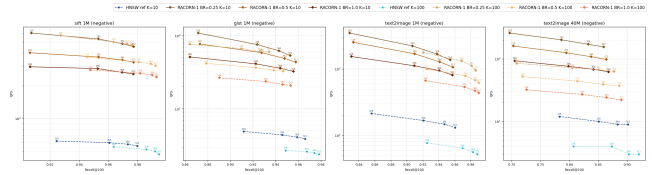


Figure 6: BR sweep under negative correlation ($K=10/100$ integrated).

BR $_{\max}$ recall gain scales with recall headroom: BR=1 \rightarrow BR $_{\max}$ recall change is SIFT 1M +0.02 (BR $_{\max}=2$), GIST 1M +0.12 (BR $_{\max}=4$), T2I 1M +0.07 (BR $_{\max}=4$), and T2I 40M +0.19 (BR $_{\max}=16$) – the largest single-step recall gain across the entire sweep. The lower the baseline recall, the larger the headroom – covered at BR $_{\max}$, at a 1.4–4.7 \times latency cost. At 0.3% and below on 1M, the BR effect tapers: RACORN-1+’s exact switch guarantees recall ≥ 0.97 from 0.3% (full 1.0 from 0.1%; §7.3), so using RACORN-1+ in this region is more effective than BR \uparrow . $EF_s \times BR$ coupling is approximately additive – at $EF_s=400 + BR=2.0$ the two effects accumulate to yield a larger recall gain than BR alone (1% GIST 0.80 \rightarrow 0.93, T2I 40M 0.70 \rightarrow 0.87, with 2–3 \times latency cost).

7.6.2 Negative Correlation BR Sensitivity (Counter-Intuitive). §7.6.1 showed under No Correlation that BR \uparrow supplies recall gain (+0.07 to +0.19) on datasets with lower baseline recall. Under §7.5’s negative correlation, the pattern reverses – this section quantifies it by sweeping RACORN-1 \times BR $\in \{0.25, 0.5, 1.0\} \times \{K = 10, K = 100\}$.

Figure 6 shows the BR sweep under negative correlation across the four datasets. At $efs=256$, **BR \downarrow emerges as the efficient frontier under negative, independent of K :** at BR=0.25 recall stays within -0.02 of BR=1.0 while latency falls to **36–52% of BR=1.0 at $K=100$ and 38–54% at $K=10$** . On SIFT $K=100$ neg, BR=0.25 (63.5 ms / 0.964) vs BR=1.0 (122.9 ms / 0.982) gives recall loss -0.018 with latency ratio 52%; the $K=10$ case mirrors this – SIFT BR=0.25 (59.6 ms / 0.953) vs BR=1.0 (111.7 ms / 0.953), recall loss 0.000, latency ratio 53%. At $K=10$ (sel $\sim 10\%$), BR \uparrow recall gain essentially vanishes (SIFT $\Delta = 0.000$, GIST $\Delta = \pm 0.005$, T2I 1M $\Delta \leq 0.003$, T2I 40M $\Delta \leq 0.012$) – a stronger “BR \downarrow efficient” signal than $K=100$ ($\sim 1\%$), because at $K=10$ the eligible-node fraction is 10% so each bridge expansion is $\sim 10\times$ more likely to discover an eligible node; recall recovers with fewer bridges. At $K=100$ the eligible nodes are sparse, so more bridges are needed and BR \uparrow shows a visible effect.

The mechanism is that under negative, fallback activates at every expansion, accumulating the per-expansion bridge cost of $\sim n \cdot b$ distance computations. Lowering BR reduces bridges per expansion while fallback itself still operates (connectivity recovery); the recall ceiling is determined not by fallback activation frequency but by **the**

eligible-region distribution reachable from bridges — hence the marginal recall gain from $BR \uparrow$ is small. This **reverses the No Correlation pattern**: §7.6.1 showed $BR \uparrow$ effective for recall on datasets with lower baseline recall (GIST 1M, T2I 40M), whereas under negative correlation $BR=0.25-0.5$ is latency-efficient. The direction of BR ’s effect flips with correlation; unified automatic BR determination across both regimes is left to future work (§8(1)). Even at $BR=0.25$, **T2I 40M neg** retains a decisive HNSW advantage: $K=100$ recall 0.81 at latency 442 ms (**20× faster than HNSW’s 8691 ms**), $K=10$ recall 0.79 at 159 ms (**20× faster than HNSW’s 3112 ms**) — for large-scale indices under negative, fractional BR is core to RACORN-1’s operational advantage over HNSW, independent of K .

7.7 Effect of HNSW Parameters on RACORN-1

RACORN-1 operates on the HNSW graph, so changes in HNSW index and search parameters (M , EF_c , EF_s) translate directly into RACORN-1 performance. Table 8 reports RACORN-1 recall × latency at 1% selectivity for the baseline and three single-parameter variants.

Table 8: RACORN-1 recall × latency at 1% selectivity (baseline: $M=16$, $EF_c=100$, $EF_s=200$).

Parameter	SIFT 1M	GIST 1M	T2I 1M	T2I 40M
baseline	0.96 / 7.5 ms	0.80 / 8.6 ms	0.84 / 7.4 ms	0.70 / 11.8 ms
$M=32$	0.97 / 9.2 ms	0.87 / 11.3 ms	0.86 / 9.6 ms	0.75 / 17.2 ms
$EF_c=500$	0.97 / 7.9 ms	0.89 / 11.0 ms	0.86 / 8.6 ms	0.74 / 13.0 ms
$EF_s=400$	0.99 / 15.0 ms	0.88 / 17.2 ms	0.92 / 14.7 ms	0.82 / 28.5 ms

Among the three HNSW parameters, **doubling M (16 → 32)** is most effective on GIST (+0.07 recall) and also gains +0.05 on T2I 40M, at the cost of 2× index memory. **Increasing EF_c (100 → 500)** has a comparable effect — significant on GIST (+0.09), moderate on T2I 40M (+0.04), and marginal on SIFT / T2I 1M (+0.01 to +0.02) — but with a 5× build-cost penalty. **Doubling EF_s (200 → 400)** is the most uniformly effective lever, delivering consistent recall improvement across all four datasets (+0.03 to +0.12) at 2.0–2.4× latency; it also activates RACORN-1+’s exact switch earlier because the AEF FB threshold scales with EF_s . GIST 1M is the dataset most responsive to all three, since index-quality reinforcement directly translates into recall in the high-dimensional setting. For T2I 40M, where the baseline 1% recall is the lowest (0.70), $EF_s = 400$ lifts it to 0.82 (+0.12 at 2.4× latency), providing a trouble-zone mitigation option.

7.8 QPS–Recall

We sweep $ef_search \in \{128, 256, 384, 512\}$ and compare the Pareto curves in the recall–QPS plane [1]. **HNSW vs RACORN-1+** (per-dataset BR; criterion: **RACORN-1+ recall at $ef=256 \geq$ HNSW@selectivity=100% recall at $ef=256 - 1\%p$ (the guardrail), maintained across all 21 selectivities**). For the QPS comparison, both algorithms are evaluated at matched $ef=256$; the four-point ef sweep is presented for the full Pareto in Figure 7.

Per-dataset guardrail and BR (Table 9; guardrail = HNSW@sel=100%@ $ef=256$ recall – 1%p; RACORN-1+ min recall is the minimum across all 21 selectivities at the chosen BR):

Table 9: Per-dataset guardrail and BR (RACORN-1+ min recall \geq guardrail).

Dataset	HNSW sel=100%	Guardrail	BR	Min recall (at sel)
SIFT 1M	0.9783	0.9683	1.5	0.9752 (2%)
GIST 1M	0.8158	0.8058	1.0	0.8069 (3%)
T2I 1M	0.9163	0.9063	2.5	0.9142 (2%)
T2I 40M	0.8051	0.7951	2.5	0.8051 (100%)

Table 10: RACORN-1+ vs HNSW QPS ratio @ matched $ef=256$ (RACORN-1+ recall maintained \geq guardrail across all selectivities; see Table 9 for per-dataset guardrails).

Selectivity band	SIFT 1M	GIST 1M	T2I 1M	T2I 40M
10–5%	2.7–5.1×	4.2–10.2×	3.6–6.3×	3.0–5.5×
3–0.5% (ASF)	6.9–7.8×	17.0–22.9×	7.8–8.6×	6.8–7.6×
0.3–0.01% (AEF, 1M)	11.1–47.6×	23.4–74.1×	13.3–58.8×	5.6–7.0×

Dynamic scaling of the AEF FB Threshold: the AEF exact-switch threshold (hereafter “AEF FB threshold”) is scaled proportionally to ef_search with $EF_s=200$ as anchor — 1M: $0.003 * (ef/200)$; 40M: $0.003 * (ef/200) * 0.1 (= 0.0003 * (ef/200))$. Across $ef \in \{128, 256, 384, 512\}$, 1M threshold ranges 0.0019–0.0077, and 40M ranges 0.00019–0.00077. This dynamic scaling generalizes to the entire ef_search sweep the two empirical observations of the §7.3 AEF FB Threshold paragraph — (i) the 1/10 ratio between 1M and 40M (cost-benefit), and (ii) proportionality to EF_s .

Table 10 consolidates the matched- ef QPS ratio across selectivity bands. Under the matched- ef QPS comparison (RACORN-1+@ $ef=256$ / HNSW@ $ef=256$), the advantage grows monotonically as selectivity falls. At 10–5% selectivity the filter-first cost cap already begins to dominate, yielding SIFT 2.7–5.1×, GIST 4.2–10.2×, T2I 1M 3.6–6.3×, and T2I 40M 3.0–5.5×. At 3–0.5% — the ASF region — the gap widens substantially: SIFT 6.9–7.8×, **GIST 17.0–22.9×**, T2I 1M 7.8–8.6×, T2I 40M 6.8–7.6×. In the AEF region on 1M (0.3–0.01%) RACORN-1+ recall reaches 1.00 and the QPS advantage scales further, with SIFT 11.1–47.6×, **GIST 23.4–74.1×**, and T2I 1M 13.3–58.8×. On T2I 40M (0.3–0.01%) the advantage is 5.6–7.0× with recall maintained \geq guardrail; the AEF brute-force cost scales with N , dampening the QPS gain relative to 1M.

8 LIMITATIONS AND FUTURE WORK

- (1) **Automatic BR determination:** this paper derives recommended BR values via static sweeps per dataset and per correlation regime (§7.5, §7.6), but production workloads exhibit query-correlation patterns and SLA priorities (recall vs latency) that vary dynamically. An integrated mechanism that continuously estimates selectivity at runtime and adaptively determines BR under SLA constraints is left as future work.
- (2) **Automatic AEF FB Threshold determination:** this paper treats it as a user-specified parameter (§5, §7.3), but the appropriate value is consistently observed to scale with both data scale N and EF_s — the N proportionality is determined by the cross-over between graph search latency

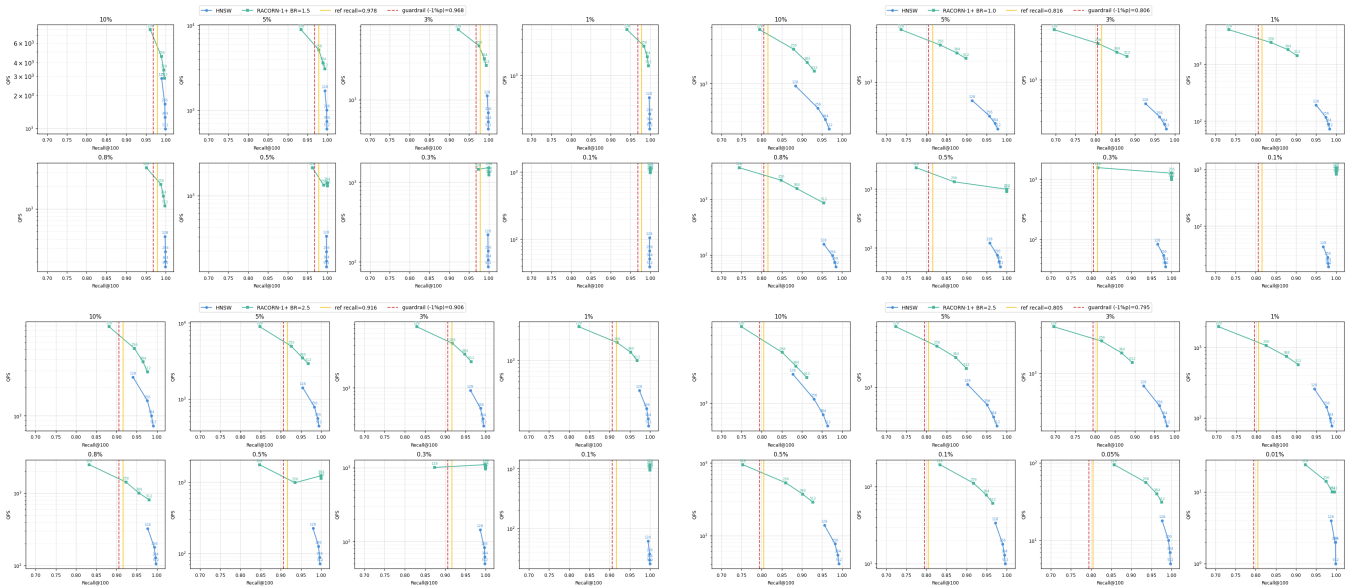


Figure 7: QPS–Recall Pareto curves at $\leq 10\%$ selectivity, HNSW vs RACORN-1+, 4-point ef sweep; yellow vertical line marks the HNSW@sel=100%@ef=256 reference.

and brute-force cost ($N \cdot s \cdot d$), yielding 1M 0.003 and 40M 0.0003, and the EF_s proportionality doubles the appropriate value when EF_s goes from 200 to 400 (the §7.8 QPS sweep validates this with $EF_s=200$ as anchor via base \cdot ef/200 dynamic scaling across $ef_search \in \{128, 256, 384, 512\}$). A closed-form derivation $\theta_{FB} = f(N, EF_s)$ or dynamic calibration from operational statistics is left as future work.

9 CONCLUSION

This work addressed the low-selectivity recall collapse of ACORN-1, the representative In-filtering algorithm, by proposing RACORN-1. Its core mechanism **Adaptive Search Fallback (ASF)** repurposes filter-failing nodes as transient bridges to reconnect severed graph paths, with stride sampling applied to bridge and two-hop candidate selection for spatial diversity. §4.4 and §4.5 develop, respectively, a region-wise cost analysis and an s -independent expansion-size lower bound under a random graph model that together formalize ASF’s connectivity preservation. ASF’s decisive contribution is empirically established by the ACORN-1 vs RACORN-1 recall delta in the §7.1 baseline (1%: +0.24 to +0.32; 0.3%: +0.74 to +0.88); §7.4 isolates stride sampling (§4.2) as a cost-free auxiliary boost. Under the baseline setting (BR=1.0, $EF_s=200$; §7.1), RACORN-1 achieves **9–26 \times latency reduction** over HNSW in the sweet spot (1%–0.3%) with a peak of **26 \times on GIST at 1%**, recovering ACORN-1’s recall collapse – 1% 0.48–0.72, 0.3% 0.03–0.10 – to 1% 0.80–0.96, 0.3% 0.87–0.98 (1M; on 40M, 1% 0.70 and 0.3% 0.77).

The newly introduced `bridge_ratio` knob enables additional recall in the ASF-activation region ($\leq 5\%$) (§7.6), supplying +0.12 to +0.19 recall gain on datasets with lower baseline recall. RACORN-1+ (RACORN-1 with AEF) handles the extreme-low-selectivity regime where graph search underperforms linear scan – at $\leq 0.1\%$ on 1M, recall 1.00 with **20–75 \times speedup**, and at 0.01% on 40M, recall 1.00

with **13 \times speedup** (§5, §7.3). The §7.8 QPS-Recall Pareto evaluation (criterion: RACORN-1+ recall \geq HNSW@sel=100%@ef=256 – 1%p at matched ef=256) reaffirms a **7–23 \times QPS advantage in the 3–0.5% ASF region and 11–74 \times in the AEF region on 1M (0.3–0.01%)**. Under adversarial query–filter correlation, §7.5 shows ACORN-1 collapsing (recall 0.08–0.41) while RACORN-1 maintains recall 0.80–0.98 with a 5–9 \times latency advantage over HNSW (§7.6.2 BR=0.25 tuning further yields up to a 20 \times speedup at T2I 40M). Together, RACORN-1 and RACORN-1+ defend recall across the extreme-low-selectivity and negative-correlation regimes where ACORN-1 fails.

REFERENCES

- [1] Martin Aumüller, Erik Bernhardsson, and Alexander Faithfull. 2020. ANN-Benchmarks: A Benchmarking Tool for Approximate Nearest Neighbor Algorithms. *Information Systems* 87 (2020), 101374. <https://arxiv.org/abs/1807.05614>
- [2] Qi Chen, Bing Zhao, Haidong Wang, Mingqin Li, Chuanjie Liu, Zengzhong Li, Mao Yang, and Jingdong Wang. 2021. SPANN: Highly-Efficient Billion-Scale Approximate Nearest Neighborhood Search. In *Advances in Neural Information Processing Systems (NeurIPS)*. <https://arxiv.org/abs/2111.08566>
- [3] Matthijs Douze, Alexandr Guzhva, Chengqi Deng, Jeff Johnson, Gergely Szilvasy, Pierre-Emmanuel Mazaré, Maria Lomeli, Lucas Hosseini, and Hervé Jégou. 2024. The Faiss Library. *arXiv preprint arXiv:2401.08281* (2024). <https://arxiv.org/abs/2401.08281>
- [4] Elastic. [n.d.]. Filtered HNSW kNN Search. <https://elastic.co/search-labs/blog/filtered-hnsw-knn-search> Elastic Search Labs.
- [5] Cong Fu, Chao Xiang, Changxu Wang, and Deng Cai. 2019. Fast Approximate Nearest Neighbor Search with the Navigating Spreading-out Graph. *Proceedings of the VLDB Endowment* 12, 5 (2019), 461–474. <https://arxiv.org/abs/1707.00143>
- [6] Siddharth Gollapudi, Neel Karia, Varun Sivashankar, Ravishankar Krishnaswamy, Nikit Begwani, Swapnil Raz, Yiyong Lin, Yin Zhang, Neelam Mahapatro, Premkumar Srinivasan, Amit Singh, and Harsha Vardhan Simhadri. 2023. Filtered-DiskANN: Graph Algorithms for Approximate Nearest Neighbor Search with Filters. In *Proceedings of the ACM Web Conference (WWW)*. <https://harshasimhadri.org/pubs/Filtered-DiskANN23.pdf>
- [7] Ruiqi Guo, Philip Sun, Erik Lindgren, Quan Geng, David Simcha, Felix Chern, and Sanjiv Kumar. 2020. Accelerating Large-Scale Inference with Anisotropic Vector Quantization. In *Proceedings of the 37th International Conference on Machine Learning (ICML)*. <https://arxiv.org/abs/1908.10396>

- [8] Hervé Jégou, Matthijs Douze, and Cordelia Schmid. 2011. Product Quantization for Nearest Neighbor Search. *IEEE Transactions on Pattern Analysis and Machine Intelligence* (2011). SIFT 1M / GIST 1M datasets: <http://corpus-texmex.irisa.fr/>.
- [9] Patrick Lewis, Ethan Perez, Aleksandra Piktus, et al. 2020. Retrieval-Augmented Generation for Knowledge-Intensive NLP Tasks. In *Advances in Neural Information Processing Systems (NeurIPS)*. <https://arxiv.org/abs/2005.11401>
- [10] J. MacQueen. 1967. Some Methods for Classification and Analysis of Multivariate Observations. In *Proceedings of the Fifth Berkeley Symposium on Mathematical Statistics and Probability*, Vol. 1. 281–297.
- [11] Yu. A. Malkov et al. [n.d.]. hnswlib: Header-only C++/Python Library for Fast Approximate Nearest Neighbors. <https://github.com/nmslib/hnswlib>
- [12] Yu. A. Malkov and D. A. Yashunin. 2018. Efficient and Robust Approximate Nearest Neighbor Search Using Hierarchical Navigable Small World Graphs. *IEEE Transactions on Pattern Analysis and Machine Intelligence* (2018). <https://arxiv.org/abs/1603.09320>
- [13] James Jie Pan, Jianguo Wang, and Guoliang Li. 2024. Survey of Vector Database Management Systems. *The VLDB Journal* 33, 5 (2024), 1591–1615. <https://arxiv.org/abs/2310.14021>
- [14] Liana Patel, Peter Kassoumeh, Carlos Guibas, et al. 2024. ACORN: Performant and Predicate-Agnostic Search Over Vector Embeddings and Structured Data. *arXiv preprint arXiv:2403.04871* (2024). <https://arxiv.org/abs/2403.04871>
- [15] Qdrant. [n.d.]. ACORN Algorithm in Qdrant 1.16. <https://qdrant.tech/blog/qdrant-1.16.x/> Qdrant Engineering Blog.
- [16] P. Griffiths Selinger, M. M. Astrahan, D. D. Chamberlin, R. A. Lorie, and T. G. Price. 1979. Access Path Selection in a Relational Database Management System. In *Proceedings of the ACM SIGMOD International Conference on Management of Data*. <https://doi.org/10.1145/582095.582099>
- [17] Harsha Vardhan Simhadri, George Williams, Martin Aumüller, et al. 2022. Results of the NeurIPS 2021 Challenge on Billion-Scale Approximate Nearest Neighbor Search. *Proceedings of Machine Learning Research* (2022). <https://arxiv.org/abs/2205.03763> Yandex Text-to-Image datasets: <https://research.yandex.com/datasets/biganns>.
- [18] Suhas Jayaram Subramanya, Devvrit, Harsha Vardhan Simhadri, Ravishankar Krishnaswamy, and Rohan Kadekodi. 2019. DiskANN: Fast Accurate Billion-Point Nearest Neighbor Search on a Single Node. In *Advances in Neural Information Processing Systems (NeurIPS)*.
- [19] Philip Sun, David Simcha, Dave Dopson, Ruiqi Guo, and Sanjiv Kumar. 2023. SOAR: Improved Indexing for Approximate Nearest Neighbor Search. In *Advances in Neural Information Processing Systems (NeurIPS)*. <https://arxiv.org/abs/2404.00774>
- [20] Unum Cloud. [n.d.]. USearch: Smaller and Faster Single-File Vector Search Engine. <https://github.com/unum-cloud/USearch>
- [21] Vespa. [n.d.]. Additions to HNSW. <https://blog.vespa.ai/additions-to-hnsw> Vespa Engineering Blog.
- [22] Jianguo Wang, Xiaomeng Yi, Rentong Guo, Hai Jin, Peng Xu, Shengjun Li, Xiangyu Wang, Xiangzhou Guo, Chengming Li, Xiaohai Xu, Kun Yu, Yuxing Yuan, Yinghao Zou, Jiquan Long, Yudong Cai, Zhenxiang Li, Zhifeng Zhang, Yihua Mo, Jun Gu, Ruiyi Jiang, Yi Wei, and Charles Xie. 2021. Milvus: A Purpose-Built Vector Data Management System. In *Proceedings of the ACM SIGMOD International Conference on Management of Data*. <https://doi.org/10.1145/3448016.3457550>
- [23] Mengzhao Wang, Lingwei Lv, Xiaoliang Xu, Yuxiang Wang, Qiang Yue, and Jiongfeng Ni. 2022. Navigable Proximity Graph-Driven Native Hybrid Queries with Structured and Unstructured Constraints. *arXiv preprint arXiv:2203.13601* (2022). <https://arxiv.org/abs/2203.13601>
- [24] Mengzhao Wang, Xiaoliang Xu, Qiang Yue, and Yuxiang Wang. 2021. A Comprehensive Survey and Experimental Comparison of Graph-Based Approximate Nearest Neighbor Search. *Proceedings of the VLDB Endowment* 14, 11 (2021), 1964–1978. <https://arxiv.org/abs/2101.12631>
- [25] Weaviate. 2024. Speed-up Filtered Vector Search. <https://weaviate.io/blog/speed-up-filtered-vector-search> Weaviate Engineering Blog.
- [26] Chuangxian Wei, Bin Wu, Sheng Wang, Renjie Lou, Chaoqun Zhan, Feifei Li, and Yuxing Cai. 2020. AnalyticDB-V: A Hybrid Analytical Engine Towards Query Fusion for Structured and Unstructured Data. *Proceedings of the VLDB Endowment* (2020). <https://doi.org/10.14778/3415478.3415541>
- [27] Chaoji Zuo, Miao Qiao, Wenchao Zhou, Feifei Li, and Dong Deng. 2024. SeRF: Segment Graph for Range-Filtering Approximate Nearest Neighbor Search. *Proceedings of the ACM on Management of Data* 2, 1 (2024), Article 69. <https://doi.org/10.1145/3639324> SIGMOD.